Nuclear Engineering and Technology 53 (2021) 949–959

Contents lists available at ScienceDirect

Nuclear Engineering and Technology

journal homepage: www.elsevier.com/locate/net

Original Article

Investigation of photon, neutron and proton shielding features of H_3BO_3–ZnO–Na_2O–BaO glass system

M.H.A. Mhareb [a, b, *], Y.S.M. Alajerami [c], Nidal Dwaikat [d], M.S. Al-Buriahi [e], Muna Alqahtani [a, b], Fatimh Alshahri [a, b], Noha Saleh [a, b], N. Alonizan [a, b], M.A. Saleh [f], M.I. Sayyed [g, h]

[a] Department of Physics, College of Science, Imam Abdulrahman Bin Faisal University, P.O. Box 1982, Dammam, 31441, Saudi Arabia
[b] Basic and Applied Scientific Research Center, Imam Abdulrahman Bin Faisal University, P.O. Box 1982, Dammam, 31441, Saudi Arabia
[c] Medical Imaging Department, Applied Medical Sciences Faculty, Al Azhar University-Gaza, Palestine
[d] Department of Physics, College of Sciences, King Fahd University of Petroleum & Minerals, Dhahran, 31261, Saudi Arabia
[e] Department of Physics, Sakarya University, Sakarya, Turkey
[f] Nuclear Engineering Programme, Faculty of Chemical and Energy Engineering, Universiti Teknologi Malaysia, Skudai, 81310, Johor, Malaysia
[g] Department of Physics, Faculty of Science, Isra University, Amman, Jordan
[h] Department of Nuclear Medicine Research, Institute for Research and Medical Consultations (IRMC), Imam Abdulrahman Bin Faisal University (IAU), Dammam, Saudi Arabia

ARTICLE INFO

Article history:
Received 1 April 2020
Received in revised form
18 July 2020
Accepted 26 July 2020
Available online 29 July 2020

Keywords:
Borate glass
Mass stopping power
Radiation shielding
Photon
Proton
Neutron

ABSTRACT

The current study aims to explore the shielding properties of multi-component borate-based glass series. Seven glass-samples with composition of (80-y)H_3BO_3–10ZnO–10Na_2O–yBaO where (y = 0, 5, 10, 15, 20, 25 and 30 mol.%) were synthesized by melt-quench method. Various shielding features for photons, neutrons, and protons were determined for all prepared samples. XCOM, Phy-X program, and SRIM code were performed to determine and explain several shielding properties such as equivalent atomic number, exposure build-up factor, specific gamma-ray constants, effective removal cross-section (Σ_R), neutron scattering and absorption, Mass Stopping Power (MSP) and projected range. The energy ranges for photons and protons were 0.015–15 MeV and 0.01–10 MeV, respectively. The mass attenuation coefficient (μ/ρ) was also determined experimentally by utilizing two radioactive sources (^{166}Ho and ^{137}Cs). Consistent results were obtained between experimental and XCOM values in determining μ/ρ of the new glasses. The addition of BaO to the glass matrix led to enhance the μ/ρ and specific gamma-ray constants of glasses. Whereas the remarkable reductions in Σ_R, MSP, and projected range values were reported with increasing BaO concentrations. The acquired results nominate the use of these glasses in different radiation shielding purposes.

1. Introduction

Radiation shielding is a method for reducing the exposure of the public and the environment to ionizing radiation. Depending on the type and energy of ionizing radiation, different materials were proposed for shielding purposes [1–6]. In numerous ways, radiation shielding is a grown technological system that is supported by a comprehensive literature form and varied computational resources. Nevertheless, improvements in our understanding of the health impact of radiation require continuous efforts to reduce these effects. Besides, the recognition of the material properties and cross-section for ionizing radiation leads to developed new substances to be applied in ionizing radiation shielding fields [1–9].

Recently, numerous researches have been performed to check the competence of different glass systems in radiation protection aspects [5,10–16]. The glass materials showed various distinctive properties such as good transparency in the visible region, chemical durability, good host for various elements, and effective atomic number. These properties make glass one of the strong candidates to be a substitute for different types of concrete used in nuclear reactors [5,10–16]. In addition to their high flexibility in fabrication, glass materials are transparent and have a good ability to absorb

* Corresponding author. Department of Physics, College of Science, Imam Abdulrahman Bin Faisal University, P.O. Box 1982, Dammam, 31441, Saudi Arabia.
E-mail address: mhsabumhareb@iau.edu.sa (M.H.A. Mhareb).

https://doi.org/10.1016/j.net.2020.07.035

Table 1
Composition ratio and density of $ZnO–Na_2O–H_3bO_3$ glass with different concentrations of BaO.

Composition ratios (mol%)	Sample Code						
	S1	S2	S3	S4	S5	S6	S7
ZnO	10	10	10	10	10	10	10
Na_2O	10	10	10	10	10	10	10
H_3BO_3	80	75	70	65	60	55	50
BaO	0	5	10	15	20	25	30
Density (g cm^{-3})	2.563	2.821	3.073	3.327	3.395	3.657	3.754

ionizing radiations like neutrons, protons, and photons based on the composition of the compound [14,17]. These glasses must own high interaction cross-section to get the ability to attenuate and absorb incident radiation [10,11].

Any glass materials utilized for ionizing radiation shielding must be steady in water and air, capable of being formed in large volumes, transparent to visible light, as well as must-have high density. Several glasses systems have been used as shielding materials for ionizing radiation such as barium borate fly ash glasses, bismuth borate glasses, silicate glasses containing (Bi_2O_3) bismuth oxide [18–20]. Borate glass has been deliberated as a result of the good thermal stability and high chemical durability such as glasses modified with heavy element oxides (Pb, Bi, and Ba) [21–23]. Also, the boron oxide has utilized to absorb the thermal neutrons and reduce secondary radiation [24]. The addition of high elements for borate glass led to increase density, enhance durability, and increase absorption of ionizing radiation [10,11,18,23]. Among the heavy elements, previous studies proved the efficiency of barium oxide (BaO) with the different glass formers in improving the

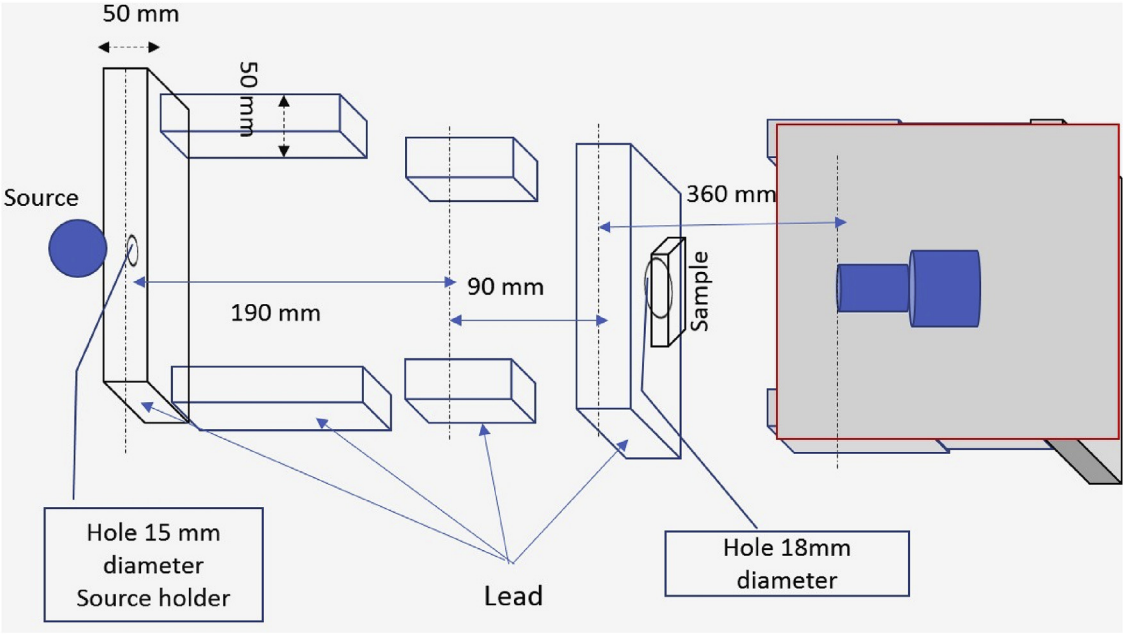

Fig. 1. Schematic view for the set-up irradiation process.

Table 2
Mass attenuation coefficients at specific energies (EXP. and XCOM).

Energy (MeV)		S1	S2	S3	S4	S5	S6	S7
0.184	EXP	0.1228	0.1396	0.1533	0.1665	0.1925	0.2161	0.2262
	XCOM	0.1265	0.1432	0.1599	0.1711	0.1977	0.2135	0.2294
	RD%	2.9244	2.5139	4.1275	2.6884	2.6302	1.2177	1.3949
0.28	EXP	0.111	0.1131	0.1254	0.1277	0.1344	0.1367	0.1335
	XCOM	0.112	0.117	0.1273	0.1249	0.1308	0.1352	0.1338
	RD%	0.8928	3.3333	1.4925	2.2417	2.7522	1.1094	0.2242
0.661	EXP	0.0734	0.0792	0.0778	0.0774	0.0776	0.0747	0.0757
	XCOM	0.0756	0.0787	0.0781	0.0778	0.0776	0.0763	0.0771
	RD%	2.9101	0.6353	0.3841	0.5141	0	2.0969	1.8158
0.71	EXP	0.0701	0.0713	0.0768	0.0742	0.0744	0.0726	0.0735
	XCOM	0.0721	0.0732	0.0755	0.0752	0.0749	0.0746	0.0742
	RD%	2.7739	2.4304	1.7218	1.3297	0.6675	2.6809	0.94339
0.81	EXP	0.0702	0.0715	0.0716	0.0723	0.0715	0.0732	0.0719
	XCOM	0.0717	0.0715	0.0709	0.0705	0.0712	0.0714	0.0701
	RD%	2.0921	0	0.9873	2.5532	0.4213	2.521	2.5677

Relative Differences (RD%) $= \frac{\mu/\rho_{\,Theor} - \mu/\rho_{\,Exp}}{\mu/\rho_{\,Theor}} \times 100.$

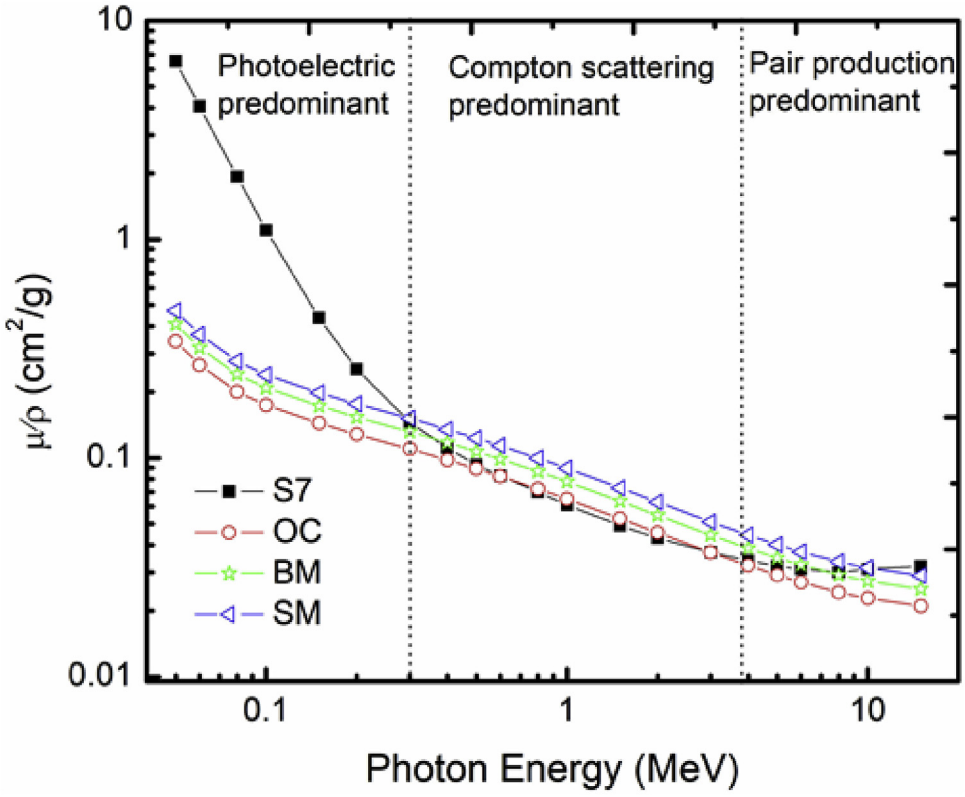

Fig. 2. Comparison of μ/ρ values of S7 and steel magnetite (SM) concretes, basalt (BM) and ordinary concrete (OC) in the energy range 0.05–15 MeV.

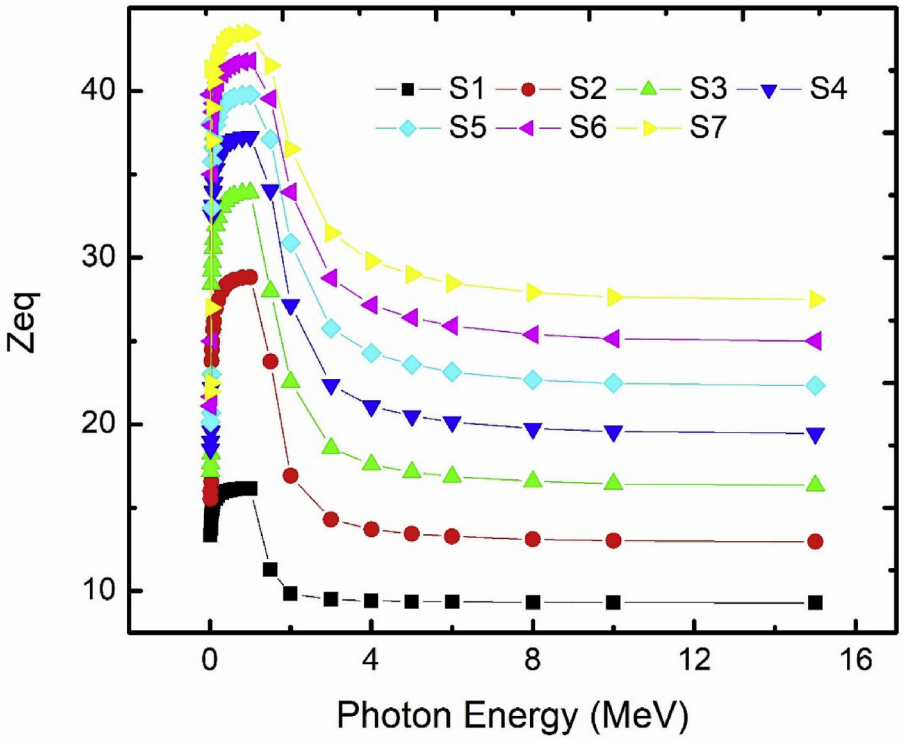

Fig. 3. The variation of Zeq for ZnO–Na_2O–H_3bO_3 glass with different concentrations of BaO with incident photon energy.

absorption of the ionizing radiations [25,26]. The addition of BaO procures to enhance the glass density as well as the atomic number, driving to the increment attenuation for photons [21]. The incorporation of sodium oxide (Na_2O) to the borate leads to change the

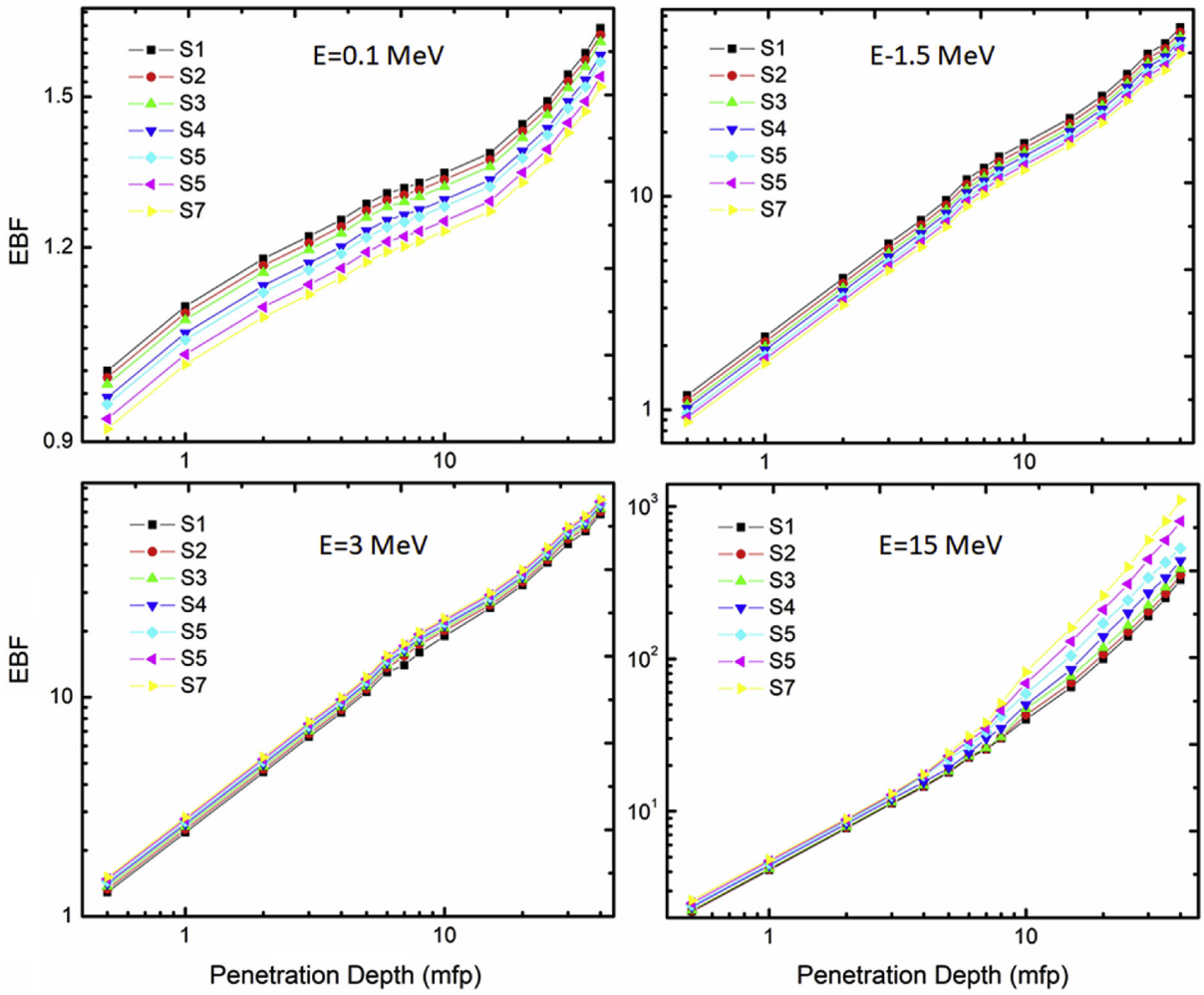

Fig. 4. Exposure buildup factor for ZnO–Na_2O–H_3bO_3 glass with different concentrations of BaO with penetration depths at specific photon energies.

boron coordination via alteration of the functional group, driving to improve the glass properties [27]. Moreover, the addendum of zinc oxide (ZnO) to borate can enhance chemical durability, thermal stability, and decreases crystallization for the glass system [28].

The present study aimed to know the effect of adding different amounts of barium oxide (BaO) on shielding properties of different types and energies of ionizing radiation such as photons, neutrons, and protons.

2. Materials and methodology

The current glass samples of nominal composition (80-y) H_3BO_3–10ZnO–10Na_2O–yBaO where y = 5, 10, 15, 20, 25, and 30 mol% were prepared by the ordinary melt-quench method. Various raw materials like boric acid (B_3BO_3), zinc oxide (ZnO), sodium oxide (Na_2O), and barium oxide (BaO) from sigma Aldrich company were utilized for preparing the current glass samples. These raw materials were weighed and mixed according to a mole percent for each element as illustrated in Table 1, after that the mixture was melted inside an electrical furnace at 1100 °C for an hour. Then the molten composition was annealed in another electrical furnace at 400 °C for 3 h to release the stress. Lastly, the electric furnace temperature was decreased progressively to room temperature with a cooling rate of 10 °C/min.

The density (ρ) values for the current samples were determined according to the Archimedes principle (see Table 1) to compute the mass attenuation coefficient (μ/ρ). The Mettler Toledo balance equipped with a specific density kit was used to determine the density values with readability 0.1 milli-gram. In this study, the experimental shielding part for calculating μ/ρ was conducted in the nuclear lab at King Fahd University of Petroleum and Minerals (KFUPM), Kingdom of Saudi Arabia (KSA). Fig. 1 illustrates the conducted irradiation set-up and detection process. Two gamma-ray sources with five different gamma energies were used to irradiate the new samples (Ho-166: 0.184, 0.280, 0.710 and 0.810 MeV; Cs-137: 0.661 MeV). The sample thickness is a critical parameter that should be adjusted to get precise irradiation. The prepared samples (with a thickness of 0.428–0.560 cm) were placed after three sequential collimation set-ups as shown in Fig. 1. To avoid the detection of background radiation, the Pb collimator set-up was adjusted to reduce the irradiation beam gradually and get the area of the glass samples. Both radiation source and detector were housed in the lead shield. Regard radiation detection, a 3x3 thallium activated sodium iodide (NaI(Tl)) scintillation detector was connected with pre-amplifier and amplifier to collect Gamma transmitted rays from irradiated samples and convert to electron counts. Gamma-ray spectrometer with a 16 K multichannel analyzer with energy resolution 7% at 662 keV was used to collect

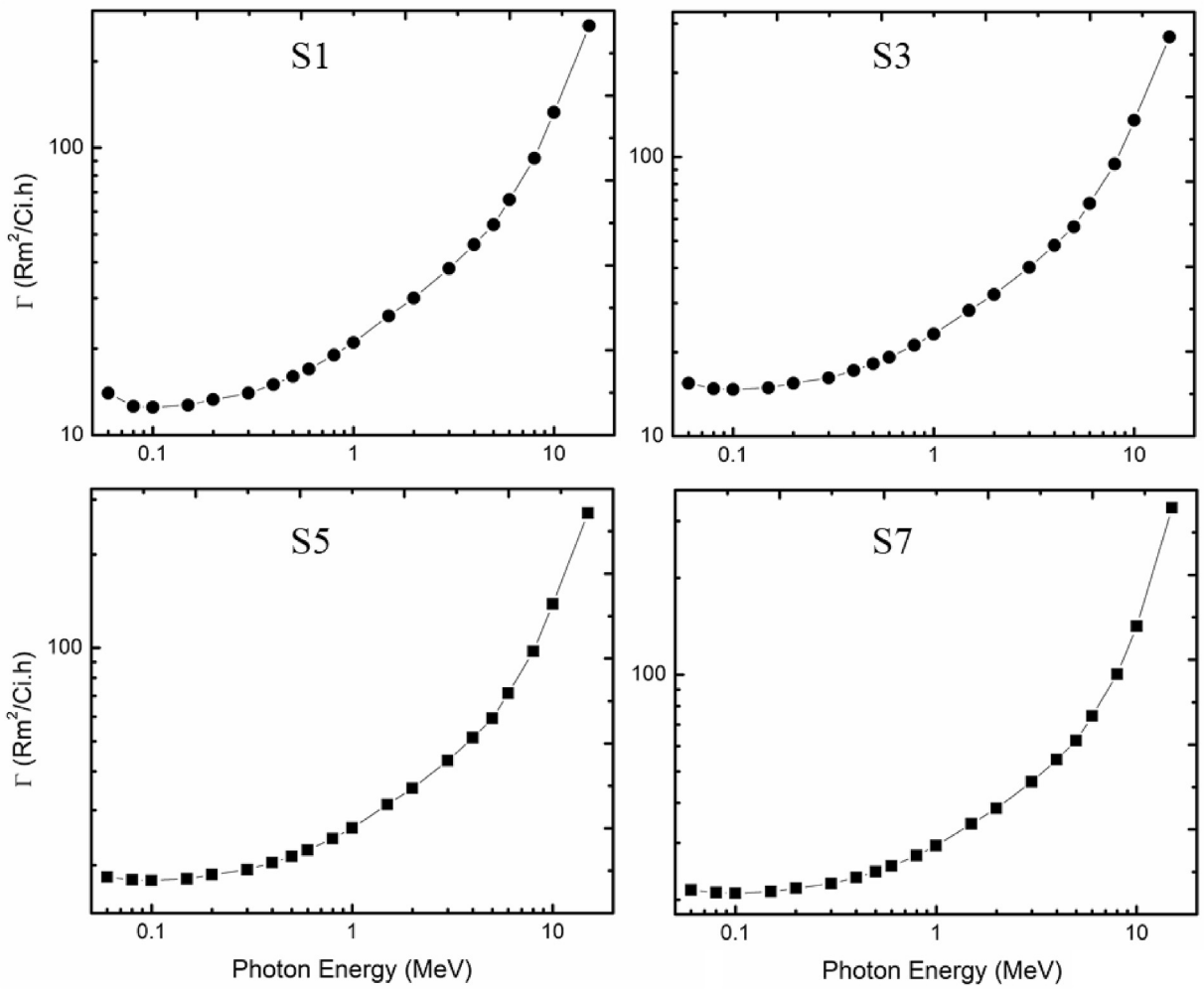

Fig. 5. Variation of the specific gamma-ray constants for ZnO–Na_2O–H_3bO_3 glass with different concentrations of BaO at different energies.

incident photon (I_o) and transmitted photons intensities (I). The distance among the radiation source and NaI scintillator detector is 64 cm for all irradiation process (either with or without samples).

The linear attenuation (μ) can be calculated according to the following formula (Lambert-Beer law) [41]:

$$I = I_0 e^{-\mu t} \tag{1}$$

Here, μ, I_o, and I denote the linear attenuation coefficient, incident, and transmitted photons, respectively. The mass attenuation coefficient of the prepared glasses can be obtained simply by dividing μ over ρ. In this study, the μ/ρ values were determined experimentally and compared with the XCOM values. XCOM is a well-common computer program designed by Breger and Hubbell [29] and developed at the National Institute of Standards and Technology (NIST/USA). This program presents the potential for computing the μ/ρ for mixtures, compounds, and elements at various photon energies (from 1 keV to 100 GeV) as well as various interactions between the photons with matter. Based on the cross-section for pair production, scattering, and photoelectric absorption, the potential of interaction was evaluated. A series of photon radiation shielding features such as an equivalent atomic number (Z_{eq}), the specific absorbed fraction of the energy (SAFE), specific gamma-ray constants (Γ) and exposure build-up factor (EBF) within the energy range of 0.015–15 MeV were also computed based on the Phy-X program [30].

Based on the mass removal cross-section of each element in the glass system, the effective removal cross-section of the fast neutron (Σ_R) was computed for each glass sample and compared with theoretical values of Phy-X results [31,32]:

$$\Sigma_R = \sum_i W_i(\Sigma_R / \rho)i \tag{2}$$

where, ρ, W_i and Σ_R denote the total density of glass sample (g cm^{-3}), the partial density (g cm^{-3}) and the mass removal cross-section of each element in the prepared glasses.

To get more shielding properties for fast neutron in the prepared glasses, neutron shielding parameters (*NSP*) such as absorption cross-sections and scattering length of the constituent elements were calculated based the following formula [33]:

$$(NSP)_{compound} = \sum f_i(NSP)i \tag{3}$$

where $(NSP)_i$ and f_i represent the neutron shielding parameters of the i^{th} element in the glass mixture and the mass fraction of each element in the glass mixtures [33]. For prepared glass samples, the following measurements were used to evaluate the absorption cross-sections and the scattering lengths of the incident neutron:

- Neutron absorption cross-section (σ_{abs})

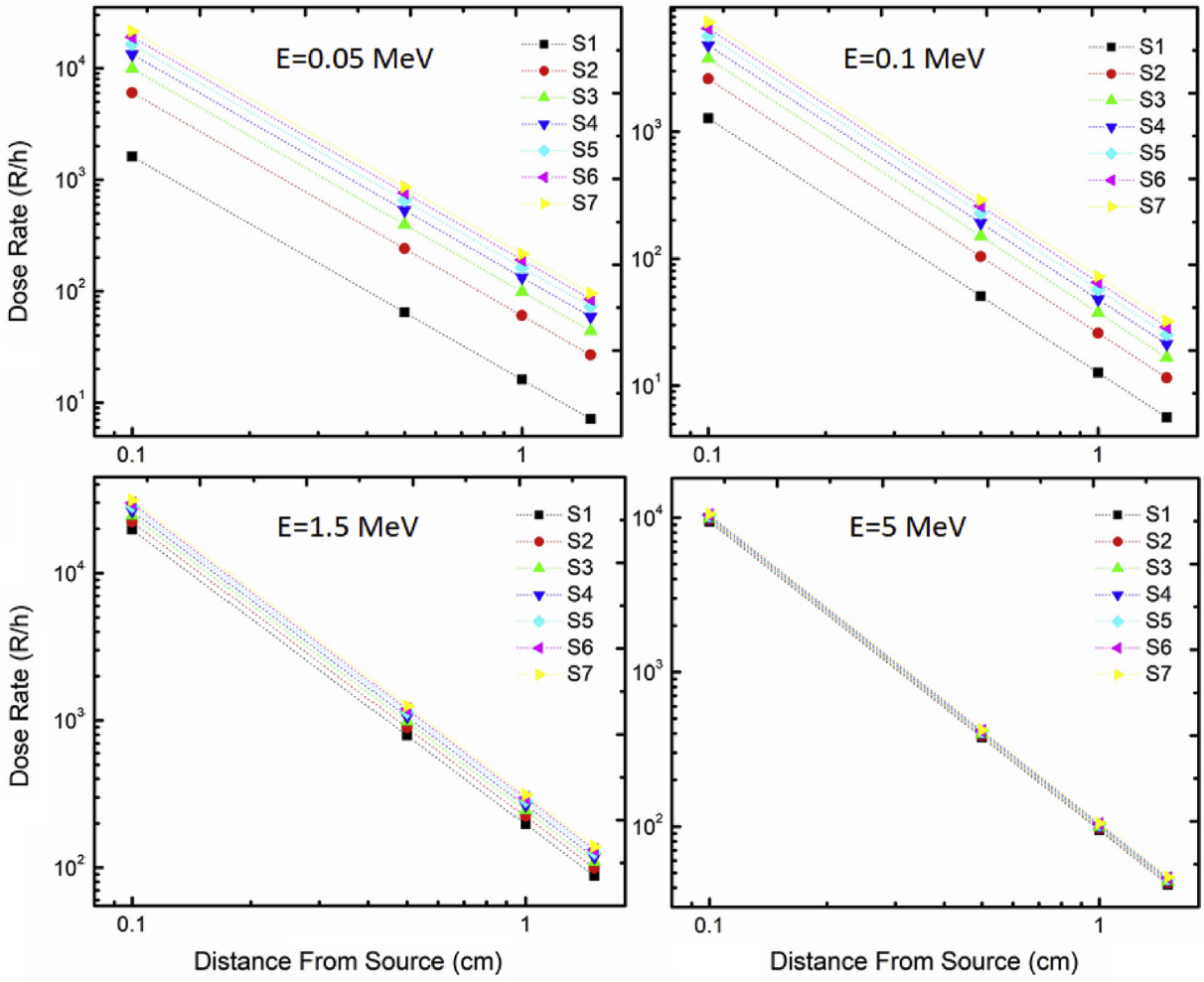

Fig. 6. Variations of gamma dose rate at different energies levels for $ZnO–Na_2O–H_3bO_3$ glass with different concentrations of BaO.

- Total neutron scattering cross-section (σ_{tot})
- Incoherent neutron scattering cross-section (σ_{inc})
- Coherent neutron scattering cross-section (σ_{coh})
- Incoherent neutron scattering length (b_{inc}),
- Coherent neutron scattering length (b_{coh}),

More particulate shielding properties such as the projected range and Mass Stopping Power (MSP) for the protons were investigated within the energy of 0.01–10 MeV based on SIRM code [34].

3. Results and discussion

Gamma-ray shielding capability of the prepared glasses was experimentally tested by evaluating μ/p employing NaI(Tl) detector at photon energies 0.184, 0.280, 0.710, and 0.810 MeV emitted from Ho-166 radioactive source, and 0.661 MeV emitted from Cs-137 radioactive source. The experimental μ/p values were compared with those of the XCOM program (theoretical side). The results of both approaches are summarized in Table 2. The experimental μ/p results come in a good agreement with the theoretical μ/p values for each prepared glass sample at the considered energy range. This harmony is good evidence that the experimental set-up has been conducted correctly. μ/p parameter is a fundamental term to recognize the capability of the material to attenuate a gamma-ray. Indeed, the measurement was repeated for each energy to minimize the errors, the background radiation was exactly determined, and all irradiation stages were executed precisely. Table 2 shows the calculated relative differences (RD) between theoretical (XCOM) and experimental results. William and Matthew reported the acceptable RD values between the experimental and theoretical results [35]. The maximum RD value among theoretical and experimental values is approximately 3%. The most dominant interactions of photons with the material are pair production interactions, Compton scattering, and the photoelectric effect. The probabilities for occurring these interactions are directly related to photon energy, atomic number, and electron density. The current glass samples consist of incorporation of various elements (see Table 1), but show the identical radiation-shielding trend, and no significant differences in μ/p are expected. However, the μ/p values revealed direct relation with the glass density, which enhanced by increasing BaO content. Furthermore, the μ/p values of the new prepared glasses were compared with some standard shielding materials such as steel magnetite (SM) concretes, basalt (BM), and ordinary concrete (OC) to explore the new glass samples that may be a good nominee for shielding purposes.

Fig. 2 shows the three fundamental interactions of gamma-ray with materials (photoelectric, Compton, and pair production) and their predominant corresponding to the incident energy. In the low energy region, the highest μ/p values can be obtained due to the dominant of the photoelectric absorption and the low occurring probability for Compton scattering. The μ/p values in this region can be sort as follow S7 > Sm > BM > OC. Consequently, the highest

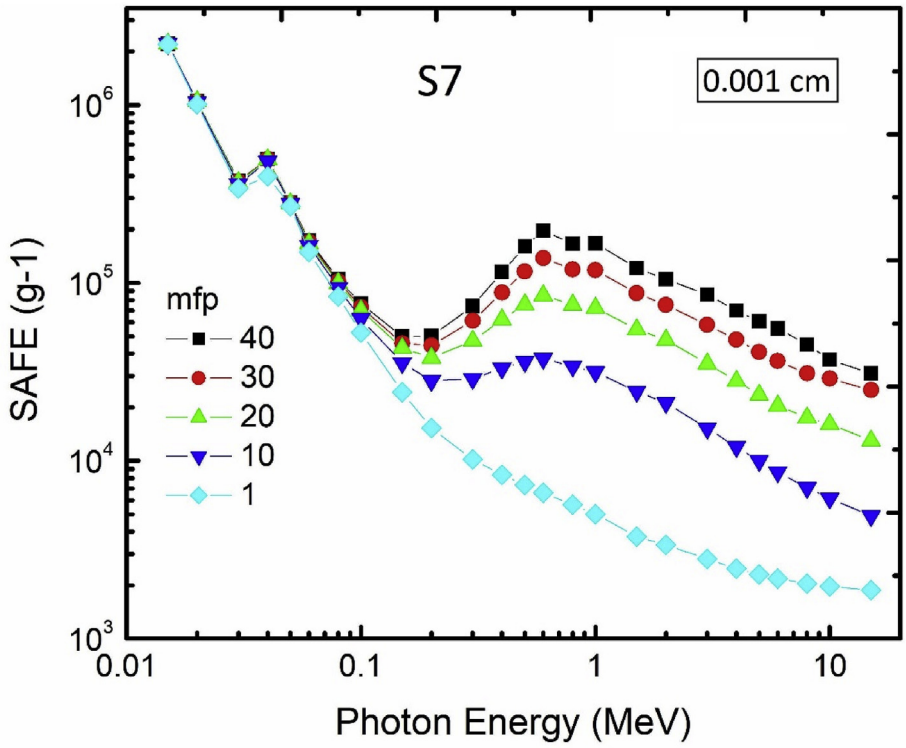

Fig. 7. The variation of SAFE with incident photon energy for S7 at 0.001 cm for different mfps.

μ/p values obtained in this region and started to reduce radically in the intermediate region (Compton scattering predominant) up to 4 MeV. The μ/p values in this region of the compared shielding materials are very close (approximately the same) and this is attributed to the independency of Compton scattering on the chemical structure of the substances. At a higher energy region (>4 MeV), the pair production probability starts to increase gradually, and the chemical structure is significant, and the materials containing heavy elements own superior shielding renderings.

From Table 2, the μ/p values at 0.184 MeV (low photon energy) were found to be maximum and they were 0.1228, 0.1396, 0.1533, 0.1665, 0.1925, 0.2161, and 0.2262 cm^2/g for S1, S2, S3, S4, S5, S6, and S7, respectively. During increasing the photon energy, the μ/p values decreased, and this is a basic trend according to the exponential attenuation equation (see Equation (1)). On the other hand, the μ/p values increased by addition BaO content at given photon energies. For example, at 0.184 MeV, the μ/p values raised from 0.1228 cm^2/g to 0.2262 cm^2/g as BaO content increased from 0 mol % to 30 mol%. Therefore, S7 glass possesses the highest μ/p values, and then it owns the best shielding ability of gamma-ray among the prepared glasses. The similar behavior of μ/p was noticed for some calcium boro-tellurite glasses [36], barium borate glasses [37], and oxyfluoro-tellurite-zinc glasses [38].

In the radiation protection context, information on photon buildup factors is essential before designing material for gamma shielding applications. This motivated us to calculate equivalent atomic number (Z_{eq}) number and then photon buildup factor (EBF and EABF) for each prepared glass sample for extended photon energy up to 15 MeV. The Z_{eq} is a parameter like the atomic number of elements, which depicts the features of the combined matter (compounds/mixture) in the expression of equivalent elements. The calculation procedures of buildup factors were explained in Refs. [39]. Furthermore, newly developed programs such as EXABCal [40] and Phy-X [30] programs can be used to obtain the results of EBF and EABF shortly and easily. The Z_{eq} results for all prepared glass samples are shown in Fig. 3. At low energy, it can be noted that the Z_{eq} values increased slightly with a peak before starting to reduce. Above 3 MeV, the values of Z_{eq} kept being nearly constant as a result of the predominance of the pair production interaction. The peak at low energy mirrored the existence of the photoelectric absorption in the K-shell electrons for heavy elements such as Zn and Ba. Moreover, the effect of BaO addition can be seen clearly in the behavior of Z_{eq} values that increased with the addition of BaO.

Fig. 4 shows the link between penetration depths and buildup factors (BUGs) for all prepared glass samples at various photon energies. The dependence on the chemical composition was observed to be vigor at the low photon energy (E_p) (E = 0.1 MeV) and the high Ep (15 MeV). However, the BUFs were independent of the chemical composition at intermediate energies such as those at 1.5 and 3 MeV. At 0.1 MeV, the highest EBF values can be seen for S1 glass, but at 15 MeV the highest EBF values were seen for S7 glass. This is attributed to the secondary particles (say photons) that deposit their energies at large mfp.

The specific gamma-ray dose constant is a radiation protection parameter used for determining the absorbed of a gamma-ray at a constant distance in a specific depth for known materials. In Fig. 5, the specific gamma-ray constants (Γ) of S1, S3, S5, and S7 are plotted for Ep up to 15 MeV. All the curves of these samples have increased with increasing incident energy. Moreover, the BaO content has a significant influence on the specific gamma-ray constants of S1, S3, S5, and S7 glasses. Such that the specific gamma-ray constants raised gradually by the increment of BaO.

The gamma dose rate (R/hr) as a function of the distance from source at energies of 0.05, 0.1, 1.5, and 5 MeV is illustrated in Fig. 6. For all prepared samples, the gamma-ray dose rate decreases with the increasing thickness of the medium. Higher dose rate reported for glasses with a high concentration BaO, and the dose rate

Table 3
The removal cross-sections and mass removal cross-section of $ZnO-Na_2O-H_3bO_3$ glass with different concentrations of BaO.

Sample Code	Element	Mass fraction	Weight Fraction	Partial Density P (g cm^{-3})	Removal Cross Section Σ_R (cm^{-1})		Mass removal Cross Section Σ_R/ρ (cm^2 g^{-1})
					Manual Calculation	Using Phys-X	
S1	H	0.3934	0.0321	0.1002	0.156	0.157	0.5980
	B	0.1311	0.1399	0.3586			0.0575
	O	0.4262	0.6665	1.7082			0.0448
	Na	0.0328	0.0792	0.1902			0.0341
	Zn	0.0164	0.0823	0.2058			0.0130
S2	H	0.3846	0.0251	0.1035	0.156	0.157	0.5980
	B	0.1282	0.1301	0.3698			0.0575
	O	0.4274	0.6395	1.7854			0.0448
	Na	0.0342	0.0788	0.2093			0.0341
	Zn	0.0171	0.0797	0.2265			0.0130
	Ba	0.0085	0.0468	0.1264			0.0129
S3	H	0.3750	0.0203	0.1051	0.155	0.156	0.5980
	B	0.1250	0.1205	0.3761			0.0575
	O	0.4286	0.5993	1.8416			0.0448
	Na	0.0357	0.0775	0.2283			0.0341
	Zn	0.0179	0.0786	0.2468			0.0130
	Ba	0.0179	0.0998	0.2750			0.0129
S4	H	0.3645	0.0158	0.1058	0.154	0.155	0.5980
	B	0.1215	0.1177	0.3783			0.0575
	O	0.4299	0.5657	1.8821			0.0448
	Na	0.0374	0.0752	0.2469			0.0341
	Zn	0.0187	0.0772	0.2668			0.0130
	Ba	0.0280	0.1444	0.4471			0.0129
S5	H	0.3529	0.0119	0.0998	0.147	0.145	0.5980
	B	0.1176	0.1075	0.3561			0.0575
	O	0.4314	0.532	1.8068			0.0448
	Na	0.0392	0.0742	0.2519			0.0341
	Zn	0.0196	0.0713	0.2723			0.0130
	Ba	0.0392	0.1997	0.6080			0.0129
S6	H	0.3402	0.0088	0.0984	0.146	0.144	0.5980
	B	0.1134	0.0941	0.3518			0.0575
	O	0.4330	0.5125	1.8230			0.0448
	Na	0.0412	0.0739	0.2713			0.0341
	Zn	0.0206	0.0699	0.2937			0.0130
	Ba	0.0515	0.239	0.8188			0.0129
S7	H	0.3261	0.0044	0.0916	0.136	0.137	0.5980
	B	0.1087	0.0884	0.3281			0.0575
	O	0.4348	0.4789	1.7452			0.0448
	Na	0.0435	0.0722	0.2785			0.0341
	Zn	0.0217	0.0684	0.3018			0.0130
	Ba	0.0652	0.2877	1.0087			0.0129

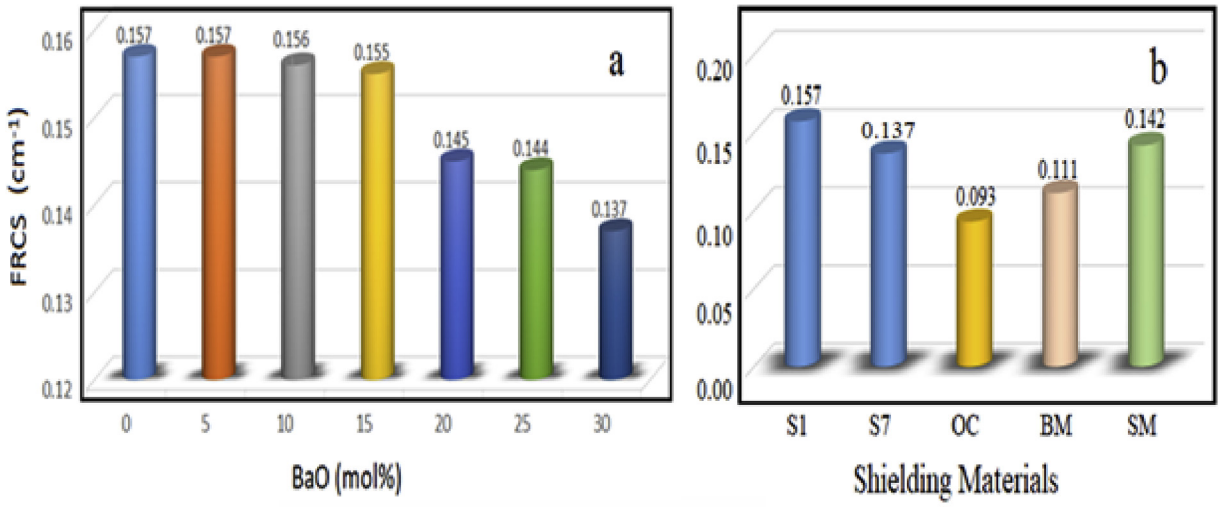

Fig. 8. Removal cross-section: a) of the prepare glasses using Phy-X, b) compare S1 and S7 with steel magnetite (SM) concretes, basalt (BM) and ordinary concrete (OC).

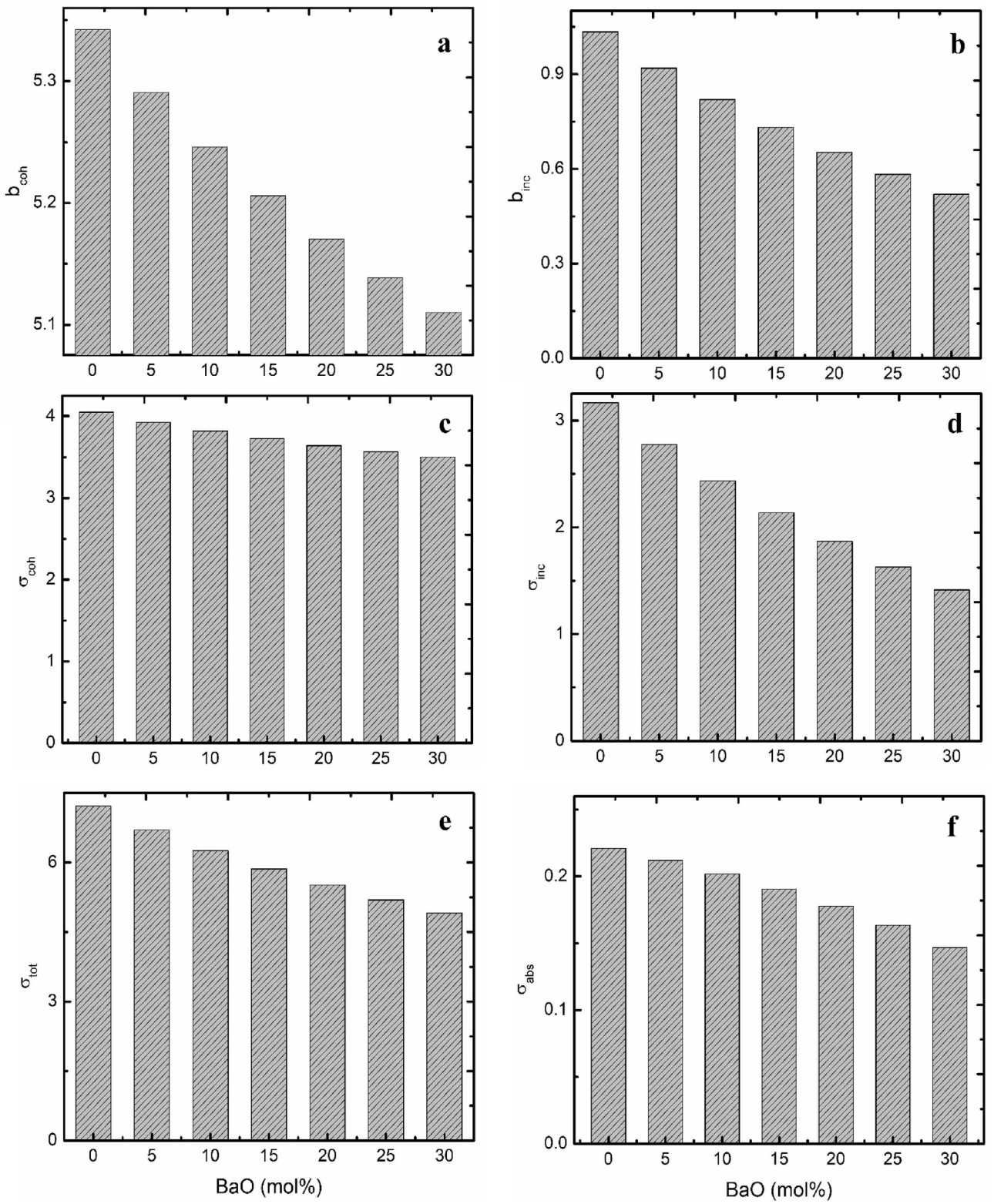

Fig. 9. The neutron absorption and scattering parameters for ZnO–Na_2O–H_3bO_3 glass with different concentrations of BaO; (a) b_{coh}: the coherent neutron scattering length, (b) b_{inc}: the incoherent neutron scattering length, (c) σ_{coh}: the coherent neutron scattering cross-section, (d) σ_{inc}: the incoherent neutron scattering cross-section, (e) σ_{tot}: the total neutron scattering cross-section, (f) σ_{abs}: the absorption neutron scattering cross-section).

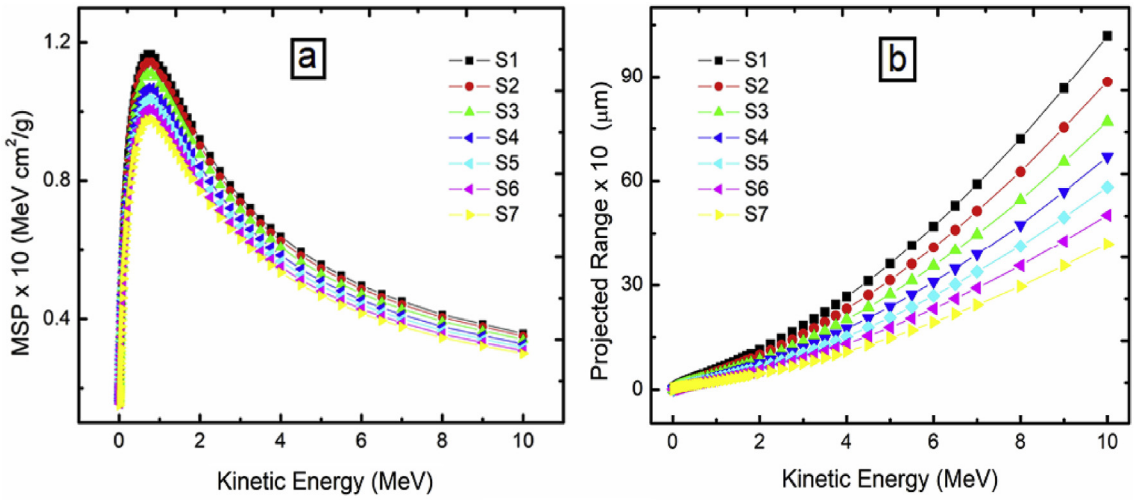

Fig. 10. Proton shielding properties for of ZnO–Na_2O–H_3bO_3 glass with different concentrations of BaO as a function of kinetic energy for: a) mass stopping power variations; b) projected range variations.

reduced by increasing BaO. Besides, it can be seen that there is an obvious difference between samples at low energy and the dose rate become almost the same at a high energy level (5 MeV).

SAFE is an essential parameter derived from the energy absorption build-up factor to determine the average absorbed dose at specific shielding materials placed at a fixed distance from the radiation source. The variation of SAFE with Ep at a thickness of 0.001 cm and up to 40 mfp for S7 glass was shown in Fig. 7. The maximum SAFE values occurred at 0.015 MeV, and then they decrease with increasing the photon energy due to the photoelectric absorption. The minimum SAFE values occurred at 15 MeV due to the dominance of pair production phenomena.

The removal cross-section of fast neutrons (Σ_R) values were calculated theoretically and obtained by using the Phy-X program for all of the prepared glasses [19]. The calculated values along with the values of Phy-X are summarized in Table 3. The calculated Σ_R values were 0.156, 0.156, 0.155, 0.154, 0.146, and 0.136 cm^{-1} for S1, S2, S3, S4, S5, S6, and S7, respectively. The Σ_R was also calculated manually, and the values are very close and showed a similar behavior when the BaO contents increase. Here, it can be noted that the neutron attenuation coefficient is inversely proportional to barium content as shown in Fig. 8(a). This trend can be ascribed to the percent mass of heavy atoms (Ba) that are predominant in the glass samples. Fig. 8(b) shows the values of Σ_R of S1 and S7 compared with some standard concrete materials. The S1 glass samples revealed higher Σ_R than SM, BM, and OC concretes. The descending order of the Σ_R values of the shielding material is S1 > SM > S7 > BM > OC. The obtained results appear that the ability of S1 to S6 glass samples to stop fast neutrons are better than the compared concretes.

Fig. 9 illustrates neutron scattering and absorption parameters (absorption neutron scattering cross-section, total neutron scattering cross-section, incoherent neutron scattering cross-section, coherent neutron scattering cross-section, incoherent neutron scattering length and coherent neutron scattering length) calculated for the new glasses [17]. The values of b_{coh}, b_{inc}, and σ_{coh} reduced with the increment of BaO content. Also, the absorption neutron scattering cross-section decreased with the increment of BaO. The values attained by S1 are ($b_{coh} = 5.410$ fm; $b_{inc} = 0.945$ fm; σ_{coh}=4.001 b and $\sigma_{abs} = 0.222$ b), which make it a possible nominee for neutron shielding implementations compared with several standard substances (concrete, graphite, and water).

Fig. 10(a) shows the values of proton mass stopping power (MSP) of the prepared glasses. As shown in the figure, the values of proton increased with increasing kinetic energy (up 1 MeV). In the energy range of 1 MeV–2 MeV, the MSP values radically decreased, and the reduction continues in the higher energies (>2 MeV) but with a low reduction rate. The sample with the highest Ba content (S7) revealed the lowest values of proton MSP. The projected range is a concept that used to define the expected depth to which alpha or proton will penetrate up to rest in an absorber material [34]. A shown in Fig. 10(b), the prepared samples, especially S7, attained low projected range values.

4. Conclusion

Seven glass samples with various concentrations of BaO were synthesized via using the melt quench method. The shielding properties of these glasses were assessed at different types and energies of ionizing radiation. The experimental results of μ/ρ exhibit good agreement with the theoretical values. The experimental values for μ/p at 0.184 MeV (low photon energy) are 0.1228, 0.1396, 0.1533, 0.1665, 0.1925, 0.2161, and 0.2262 cm^2/g for S1, S2, S3, S4, S5, S6, and S7, respectively. While the values of Σ_R for S1, S2, S3, S4, S5, S6, and S7 are 0.156, 0.156, 0.155, 0.154, 0.146, and 0.136 cm^{-1}, respectively. The results revealed that by increasing BaO contents the density, μ/ρ, and specific gamma-ray constants improved and inversely effects on Σ_R, MSP, and projected range values. The current results proved the ability of the new glasses to be good shielding material in different ionizing radiation facilities.

Declaration of competing interest

The authors declare that they have no known competing financial interests or personal relationships that could have appeared to influence the work reported in this paper.

Acknowledgment

The authors gratefully acknowledge the use of the services and facilities of the Basic and Applied Scientific Research Center at Imam Abdulrahman Bin Faisal University and the authors also wish to thank Dr. Nidal Dwaikat who designed the gamma-ray irradiation system and carried out the experimental part in the Physics department at KFUPM.

Appendix A. Supplementary data

Supplementary data related to this article can be found at https://doi.org/10.1016/j.net.2020.07.035.

References

[1] Ju Hyuk Lee, Hyun Nam Kim, Heon Yong Jeong, Sung Oh Cho, Optimization of shielding to reduce cosmic radiation damage to packaged semiconductors during air transport using Monte Carlo simulation, Nucl. Eng. Technol. 52 (2020) 1817–1825/.

[2] Tayfun Bel, Cuneyt Arslan, Nilgun Baydogan, Radiation shielding properties of poly (methyl methacrylate)/colemanite composite for the use in mixed irradiation fields of neutrons and gamma rays, Mater. Chem. Phys. 221 (2019) 58–67.

[3] M. Kh Hamad, M.H.A. Mhareb, Y.S. Alajerami, M.I. Sayyed, Gameel Saleh, Y. Maswadeh, KhA Ziq, Radiation shielding properties of Nd0.6Sr0.4Mn1−yNiyO3 substitute with different concentrations of nickle, Radiat. Phys. Chem. 174 (2020) 108920.

[4] Y. Al-Hadeethi, M.I. Sayyed, Hiba Mohammed, Lia Rimondin, X-ray photons attenuation characteristics for two tellurite based glass systems at dental diagnostic energies, Ceram. Int. 46 (2020) 251–257.

[5] Kawa M. Kaky, M.I. Sayyed, M.H.A. Mhareb, Alyaa H. Abdalsalam, K.A. Mahmoud, S.O. Baki, M.A. Mahdi, Physical, structural, optical and gamma radiation attenuation properties of germanate-tellurite glasses for shielding applications, J. Non-Cryst. Solids 545 (2020) 120250.

[6] M.I. Sayyed, Alyaa H. Abdalsalam, Malaa M. Taki, M.H.A. Mhareb, Bünyamin Alim, Baltakesmez Ali, Erdem Şakar, MoO3 reinforced Ultra high molecular weight PE for neutrons shielding applications, Radiat. Phys. Chem. 172 (2020) 108852.

[7] J. Luković, B. Babić, D. Bučevac, M. Prekajski, J. Pantić, Z. Baščarević, B. Matović, Synthesis and characterization of tungsten carbide fine powders, Ceram. Int. 41 (2015) 1271–1277, https://doi.org/10.1016/j.ceramint.2014.09.057.

[8] J.K. Shultis, R.E. Faw, Radiation shielding technology, Health Phys. 88 (2005) 587–612.

[9] O. Agar, M.I. Sayyed, F. Akman, H.O. Tekin, M.R. Kaçal, An extensive investigation on gamma ray shielding features of Pd/Ag-based alloys, Nucl. Eng. Technol. 51 (2019) 853–859.

[10] V.P. Singh, N.M. Badiger, N. Chanthima, J. Kaewkhao, Evaluation of gamma-ray exposure buildup factors and neutron shielding for bismuth borosilicate glasses, Radiat. Phys. Chem. 98 (2014) 14–21, https://doi.org/10.1016/j.radphyschem.2013.12.029. Elsevier.

[11] P. Kaur, D. Singh, T. Singh, Heavy metal oxide glasses as gamma rays shielding material, Nucl. Eng. Des. 307 (2016) 364–376.

[12] V.P. Singh, N.M. Badiger, J. Kaewkhao, Radiation shielding competence of silicate and borate heavy metal oxide glasses: comparative study, J. Non-Cryst. Solids 404 (2014) 167–173, https://doi.org/10.1016/j.jnoncrysol.2014.08.003. Elsevier B.V.

[13] M. Mariyappan K. Marimuthu, M.I. Sayyed, M.G. Dong, U. Kara, Effect Bi2O3 on the physical, structural and radiation shielding properties of Er3+ ions doped bismuth sodium fluoroborate glasses, J. Non-Cryst. Solids 499 (2018) 75–85.

[14] M.H.A. Mhareb, Physical, optical and shielding features of Li2O-B2O3-MgO-Er2O3 glasses co-doped of Sm2O3, Appl Phys-A Mater. 126 (2020) 71.

[15] El-Mallawany, M.I. Sayyed, Comparative shielding properties of some tellurite glasses: part 1, Phys. B Condens. Matter 539 (2018) 133–140.

[16] El-Mallawany, M.I. Sayyed, Comparative shielding properties of some tellurite glasses: part 1, Phys. B Condens. Matter 539 (2018) 133–140.

[17] Y.S. Alajerami, D. Drabold, M.H.A. Mhareb, K.L.A. Cimatu, G. Chen, M. Kurudirek, Radiation shielding properties of bismuth borate glasses doped with different concentrations of cadmium oxides, Ceram. Int. 46 (2020) 12718–12726.

[18] M. Kurudirek, N.A. Chutithanapanon, R.A. Laopaiboon, C.H. Yenchai, C.H. Bootjomchai, Effect of Bi2O3 on gamma ray shielding and structural properties of borosilicate glasses recycled from high pressure sodium lamp glass, J. Alloys Compd. 745 (2018) 355–364, https://doi.org/10.1016/j.jallcom.2018.02.158. Elsevier B.V.May.

[19] K.M. Kaky, M.I. Sayyed, Abbas Khammas, Ashok Kumar, Erdem Şakar, Alyaa H. Abdalsalam, Betül Cevïz Şakar, Bünyamin Alim, M.H.A. Mhareb, Theoretical and experimental validation gamma shielding properties of B2O3–ZnO–MgO–Bi2O3 glass system, Mater. Chem. Phys. 242 (2020) 122504.

[20] C.K. Mahapatra, S.V. Barai, Hybrid fiber reinforced self compacting concrete with fly ash and colloidal nano silica : a systematic study, Construct. Build. Mater. 160 (2018) 828–838, https://doi.org/10.1016/j.conbuildmat.2017.11.131. Elsevier Ltd.

[21] M.H.A. Mhareb, Muna Alqahtani, Fatimh Alshahri, Y.S.M. Alajerami, Noha Saleh, N. Alonizan, M.I. Sayyed, et al., The impact of barium oxide on physical, structural, optical, and shielding features of sodium zinc borate glass, J. Non-Cryst. Solids 541 (2020) 120090.

[22] K. Kirdsiri, J. Kaewkhao, A. Pokaipisit, W. Chewpraditkul, P. Limsuwan, Gamma-rays shielding properties of xPbO:(100−x) B2O3 glasses system at 662 keV, Ann. Nucl. Energy 36 (9) (2009) 1360–1365.

[23] E.R. Shaaban, M. Shapaan, Y.B. Saddeek, Structural and thermal stability criteria of Bi2O3–B2O3 glasses, J. Phys. Condens. Matter 20 (15) (2008) 155108.

[24] F. Gaber, M. El-Sarraf, W. Kansouh, Utilization of boron oxide glass and epoxy/ilmenite assembly as two layer shield, Ann. Nucl. Energy 57 (2013) 106–110.

[25] R. Bagheri, A.K. Moghaddam, H. Yousefnia, Gamma ray shielding study of bariume-bismuthe-borosilicate glasses as transparent shielding materials using MCNP-4C code, XCOM program, and available experimental data, Nucl. Eng. Technol. 49 (2017) 216–223.

[26] S. Sukhpal, A. Kumar, D. Singh, K.S. Thind, G.S. Mudahar, Barium–borate–flyash glasses: as radiation shielding materials, Nucl. Instrum. Methods B 266 (2008) 140–146.

[27] N.A. Razak, S. Hashim, M.H.A. Mhareb, Y.S.M. Alajerami, S.A. Azizan, N. Tamchek, Impact of Eu3+ ions on physical and optical properties of Li2O-Na2O-B2O3 glass, Chin, J. Chem. Phys. 29 (3) (2016) 395.

[28] Mohd Zaid, Mohd Hafiz, et al., Effect of ZnO on the physical properties and optical band gap of soda lime silicate glass, Int. J. Mol. Sci. 13 (2012) 7550–7558.

[29] M.J. Berger, J.H. Hubbell, XCOM: Photon Cross Sections on a Personal Computer. No. NBSIR-87-3597, National Bureau of Standards, Washington, DC (USA), 1987. Center for Radiation Research.

[30] E. Şakar, Ö.F. Özgür, A. Bünyamin, M.I. Sayyed, M. Kurudirek, Phy-X/PSD: development of a user friendly online software for calculation of parameters relevant to radiation shielding and dosimetry, Radiat. Phys. Chem. 166 (2020) 108496.

[31] M.F. Kaplan, Concrete Radiation Shielding, John Wiley and Sons., New York, USA, 1989.

[32] J. Wood, Computational Methods in Reactor Shielding, Pergamon Press, Inc., New York, USA, 1982.

[33] V.F. Sears, Neutron scattering lengths and cross section, Neutron News 3 (3) (1992) 26–37.

[34] J.F. Ziegler, M.D. Ziegler, J.P. Biersack, SRIM - the stopping and range of ions in matter, Nucl. Instrum. Methods B 268 (2010) 1818–1823.

[35] L. William Oberkampf, Matthew F. Barone, Measures of agreement between computation and experiment: validation metrics, J. Comput. Phys. 217 (1) (2006) 5–36.

[36] M.S. Al-Buriahi, M.I. Sayyed, Y. Al-Hadeethi, Role of TeO2 in radiation shielding characteristics of calcium boro-tellurite glasses 46 (2020) 13622–13629.

[37] M.S. Al-Buriahi, C. Sriwunkum, A. Halil, T.T. Baris, A.B. Mohamed, Investigation of barium borate glasses for radiation shielding applications, Appl Phys-A Mater. 126 (1) (2020) 1–9.

[38] M.I. Sayyed, A. Hakan, M.S. Al-Buriahi, L. Eloic, A. Rachid, B. Giovanni, Oxy-fluoro-tellurite-zinc glasses and the nuclear-shielding ability under the substitution of AlF3 by ZnO, Appl Phys-A Mater. 126 (2) (2020) 1–12.

[39] American National Standard, Gamma-Ray Attenuation Coefficients and Buildup Factors for Engineering Materials, 1991. ANSI/ANS-6.4.3.

[40] I.O. Olarinoye, R.I. Odiaga, S. Paul, EXABCal: a program for calculating photon exposure and energy absorption buildup factors, Heliyon 5 (2019), e02017.

[41] Volodymyr Mosorov, The Lambert-Beer law in time domain form and its application, Appl. Radiat. Isot. 128 (2017) 1–5, https://doi.org/10.1016/j.apradiso.2017.06.039.